Available online at www.sciencedirect.com
SCIENCE DIRECT®

Journal of the European Ceramic Society 24 (2004) 1171–1175
www.elsevier.com/locate/jeurceramsoc

Ceramic varistors based on ZnO–SnO_2

A. Anastasiou, M.H.J. Lee, C. Leach, R. Freer*

Manchester Materials Science Centre, University of Manchester and UMIST, Manchester M1 7HS, UK

Abstract

Model ceramic varistor formulations based on 98% ZnO–SnO_2 (plus 2% oxides of Bi, Co and Mn) were prepared by conventional powder processing routes; specimens were sintered at 1150–1275 °C. The product density increased with SnO_2 content, but decreased with increase in sintering temperature. The microstructures contained ZnO, Zn_2SnO_4 spinel and very small bismuth rich phases; with increasing Sn content the spinel became the dominant phase. From I–V measurements, the non-linear coefficients were found to be in the range 24–32. For all compositions, the α values decreased with increasing sintering temperature; the maximum α value was obtained with samples containing 20 mol% SnO_2 sintered at 1200 °C. Breakdown fields were in the range 3000–11000 V/cm and increased with increasing tin content. Leakage currents were in the range 1–11 μA. Tin substitution for Zn appears to cause a strong donor effect.

Keywords: Grain boundary; Non-linear coefficient; Varistors; ZnO

1. Introduction

Varistors[1] are materials with unique non-linear, current–voltage characteristics that allow them to be employed in voltage surge protection applications. Today, the majority of varistors produced commercially are based on ZnO with minor additions[2] of typically Bi_2O_3, Sb_2O_3, CoO, MnO_2 and Cr_2O_3. The minor constituents segregate to the grain boundaries to help develop barriers to electrical conduction, and also form spinel phases $Zn_7Sb_2O_{12}$ at triple points and grain boundaries. The double, back-to-back Schottky barriers at the grain boundaries are the primary reason for the non-linear current–voltage (I–V) behaviour; the latter may conveniently be described in terms of a non-linear coefficient α (which is defined by $I = KV^{\alpha}$, where K is a constant of proportionality). For a good quality ZnO based varistor, the non-linear coefficient is typically 40–50.

In recent years there has been growing interest in varistors of alternative formulations and these have included base compositions of tungsten oxide,[3] $SrTiO_3$,[4] and TiO_2.[5–7] Such varistors tend to exhibit comparatively small α values (generally in the range 2–12) which limits their commercial exploitation, but SnO_2 based varistors[8,9] have emerged as one of the few novel systems where α values in excess of 40 have been achieved. Additions of CoO to SnO_2 are reported to yield high-density products[8] but such varistors are not as easy to fabricate as the classical ZnO based products. Recently, Bernik and Daneu[10] prepared ZnO varistors (of commercial formulation) where the Sb_2O_3 component (total 1 mol%) was systematically replaced by SnO_2. They observed a significant increase in leakage current and increase in donor density with SnO_2 doping. In the present study we have examined microstructure development and the electrical characteristics of a model system based on ZnO (plus Bi_2O_3, Mn_2O_3, and Co_2O_3) where the ZnO was systematically replaced by SnO_2 (up to 20 mol%).

2. Experimental

Samples with nominal compositions (98–x)ZnO–$x$$SnO_2$ (plus 0.5% Bi_2O_3, 0.5% Mn_2O_3 and 1.0% Co_2O_3; all in mol%) where $x = 0$, 5.0, 10.0, 15.0, 17.5 and 20 mol%, were produced by the mixed oxide route using powders of 99.0–99.9% purity. For each composition, the powders were mixed in appropriate

* Corresponding author. Tel.: +44-161-200-3564; fax: +44-161-200-3586.
E-mail address: robert.freer@umist.ac.uk (R. Freer).

0955-2219/$ - see front matter © 2003 Elsevier Ltd. All rights reserved.
doi:10.1016/S0955-2219(03)00472-2

proportions and milled with propan-2-ol, using zirconia media for periods up to 24 h. After drying, the powders were pressed into discs (12 mm diameter, 2 mm thick) and fired at temperatures in the range 1150–1275 °C for 1 h. The heating and cooling rate was 4 °C/min.

Specimen densities were determined from weight and dimension measurements. The phases present were identified by X-ray diffraction (XRD) techniques (Philips X'Pert system) using Cu K_α radiation. For microstructure analysis, sintered products were ground and polished down to 1 μm diamond paste. Selected samples were etched either thermally (by heating rapidly to 200 °C below the sintering temperature and holding for 10 min) or by the use of dilute acid (5% hydrochloric acid for 5–10 s). Morphologies were examined optically and by scanning electron microscopy (SEM) using Philips 505 SEM equipped with energy dispersive spectrometer. Grain sizes were determined by the linear intercept method. Second phases were examined by transmission electron microscopy (TEM using a Philips EM430). Samples were mechanically thinned and ion beam thinned using an ION TEC 791 ion beam thinner.

For electrical measurements the specimen thickness was reduced to 0.5–1.0 mm and silver electrodes applied to both sides of the discs. Each specimen was fired at 550 °C for 60 min, using 4 °C/min heating and cooling rates. DC–measurements were undertaken using a Brandenburg power supply (475A) in conjunction with digital multimeters (Fluka 8012A). The non-linear coefficient α was determined across the current density range 0.1–1.0 mAcm^2 via the relationship

$$\alpha = (\log J_2 - \log J_1)/(\log E_2 - \log E_1) \quad (1)$$

where J_2 and J_1 are current densities at applied electric fields E_2 and E_1. The breakdown fields E_b were determined at current densities of 0.5 mA/cm^2. The leakage current I_L was determined at 0.75 E_b.

3. Results and discussion

Good quality, high-density products were obtained for sintering temperatures of 1200 °C or higher. Fig. 1 summarises densification behaviour of the specimens as a function of sintering temperature. With increasing substitution of ZnO by SnO_2, the density increases as a greater proportion of the heavier element is incorporated into the samples. However, independently of composition, the density tends to decrease with increasing sintering temperature, probably due to evaporation of ZnO at the higher temperatures.

Typical examples of the microstructures for samples sintered at 1250 °C are presented in Fig. 2. At low levels of SnO_2 substitution (up to 5%) the microstructure is still dominated by large ZnO grains (about 10 μm in size) exhibiting inversion boundaries with spinel phases

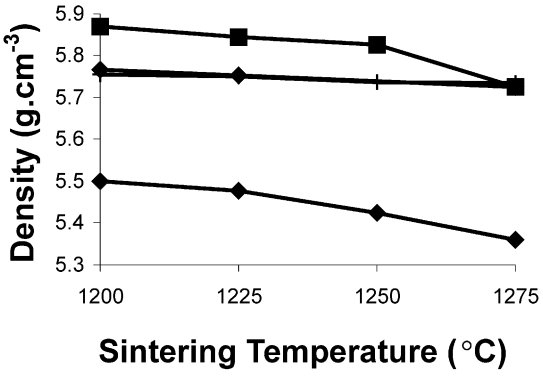

Fig. 1. Specimen density as a function of sintering temperature for samples prepared with different amounts of SnO_2 (◆ 5%, | 15%, ▲ 17.5%, ■ 20%).

at triple points and along ZnO grain boundaries. Although the sintering temperature had little effect on grain size, there were significant changes in microstructure and grain size with specimen composition. As SnO_2 replaced the ZnO there was a rapid increase in the amount of the second phase and a distinct decrease in the size of the ZnO grains. Simple image analysis of the microstructures suggested that the second phase constituted approximately 35% of the samples when the SnO_2 content was 5% (Fig. 2b), but the "second phase" fraction increased to almost 60% when the SnO_2 content in the starting mixture was 20% (Fig. 2d). Clearly the tin rich second phase effectively pins the grain boundaries, limiting the growth of ZnO grains. It is also evident that whilst there are many small second phase grains, the second phase was able to grow rapidly to individual and aggregated grains of 20 μm or larger.

The microstructures for these ZnO–SnO_2 ceramics are in marked contrast to those of (1) the SnO_2 based ceramics,[8,9] where there is predominantly a monophase microstructure of relatively uniform size, and (2) the classical ZnO based systems, where the primary grains still dominate the Zn–Sb spinel second phases.[11] In the related study of Bernik and Daneu[10] the initial 1% Sb_2O_3 was systematically replaced by SnO_2. They found very little change in grain size (all ZnO grains around 11.5 μm) and the second phase was small in size and volume, being primarily confined to triple points and grain boundaries. However, as the Sb/Sn ratio changed in the starting mixtures, there was a clear change in the nature and composition of the spinel phase ($Zn_7Sb_2O_{12}$ and/or Zn_2SnO_4) and occasionally traces of pyrochlore were detected. As the 'model' composition used in this study did not include Sb_2O_3 the resulting phase development was much simpler than that reported by Bernik and Daneu.[10] EDS analysis of the second phases in Fig. 2 confirmed the presence of only one type of spinel, Zn_2SnO_4, and these contained small amounts of cobalt and manganese. Indeed XRD spectra for all the Sn-bearing samples revealed only two phases, ZnO and

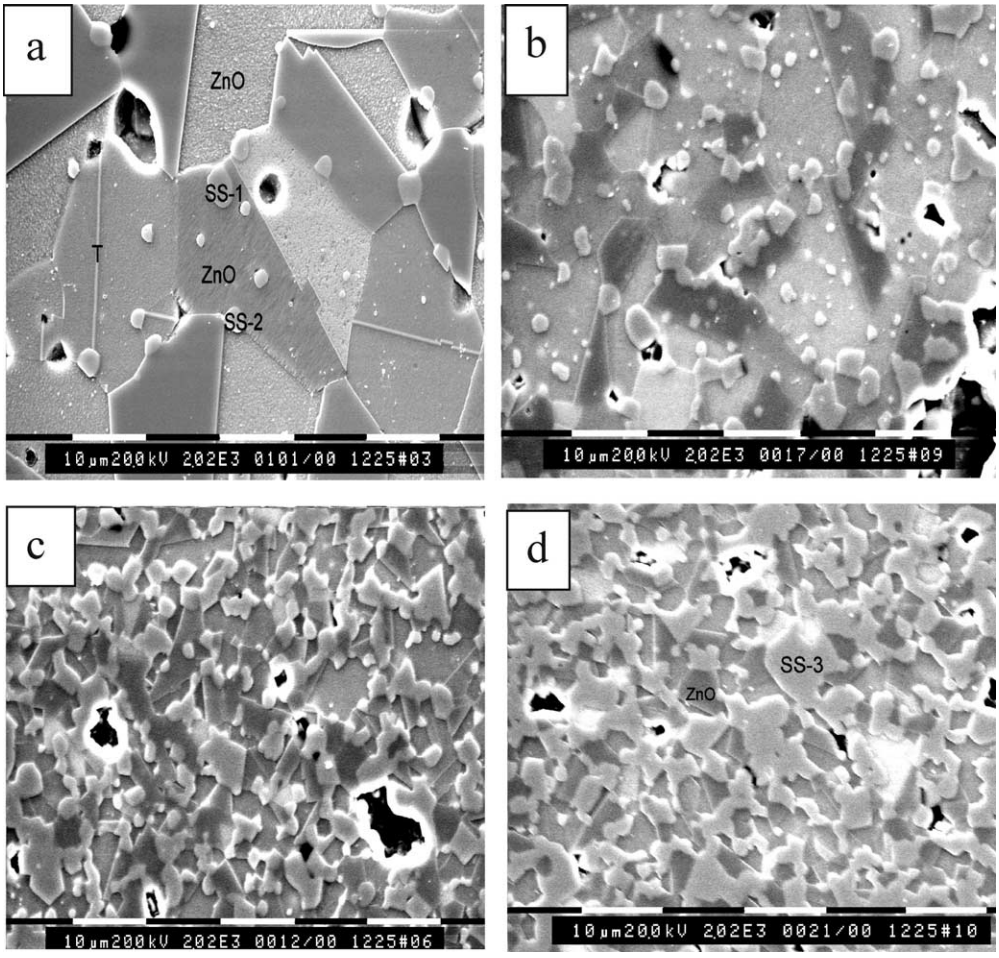

Fig. 2. SEM micrographs of specimens prepared with different amounts of SnO_2: (a) 1%, (b) 5%, (c) 15%, (d) 20%. SS denotes second phase grains.

Zn_2SnO_4; as the Sn content increased the intensity of the spinel peaks grew at the expense of the ZnO peaks. Limited TEM analysis confirmed the presence of Bi_2O_3-rich phases along the grain boundaries. These tended to be in the shape of laths and predominantly of bismuth oxide in composition, with small amounts of cobalt and manganese. In the presence of the very strong peaks for ZnO and Zn_2SnO_4 it was not possible to detect the bismuth rich phases by XRD.

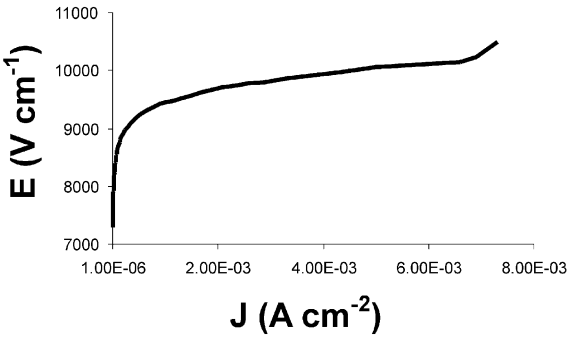

Fig. 3. Electric field current density (E–J) profile for sample prepared with 20% SnO_2 sintered at 1275 °C.

Due to the high resistivity of the specimens, it was necessary to reduce specimen thickness below 1 mm in order to perform I–V measurements. A typical I–V profile is shown in Fig. 3. In some samples there was a suggestion that the I–V profile included part of the pre-breakdown region (as in Fig. 3), but most terminated in the non-linear region. Using Eq. (1) the non-linear coefficients (α) were determined; results are presented in Fig. 4. There is a clear dependence of α values on sample composition and sintering temperature. With increasing SnO_2 content, particularly above 15%, there is a small increase in α value; this in part reflects the improvement in densification (Fig. 1). If this trend continues then significantly higher α values would be expected in the SnO_2 based varistors. Indeed for SnO_2 varistors containing small amounts of CoO, Cr_2O_3, Ta_2O_5, non-linear coefficients in excess of 40 have been reported.[8,9] For the ZnO–SnO_2 samples in the present study, the non-linear coefficients decrease, almost linearly with increasing sintering temperature (reflecting the decrease in density). At 1200 °C the maximum α values of 28–32 were achieved, with the highest value being that for samples prepared with 20% SnO_2. In the SnO_2-

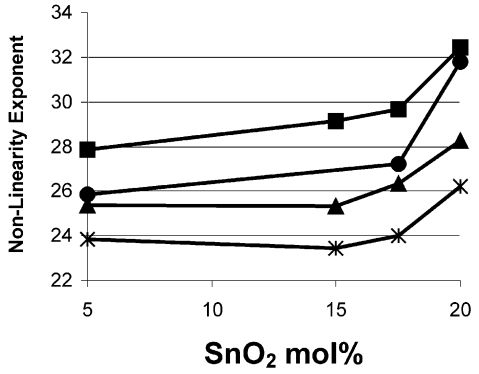

Fig. 4. Non-linear exponent as a function of SnO_2 content (and sintering temperature: ■ 1200 °C, ● 1225 °C, ▲ 1250 °C, ∗ 1275 °C).

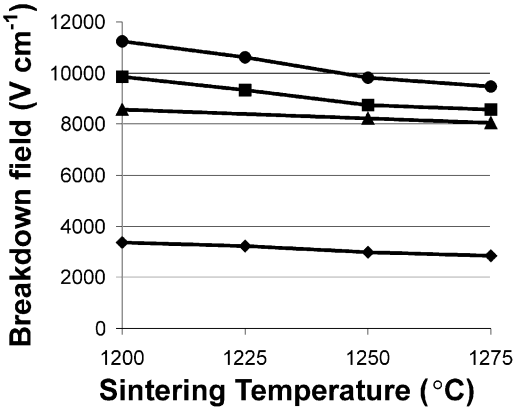

Fig. 5. Breakdown field as a function of sintering temperature for samples prepared with different amounts of SnO_2 (◆ 5%, ▲ 15%, ■ 17.5%, ● 20%).

doped ZnO varistors, Bernik and Daneu,[10] found that the low levels of tin oxide (up to 1 mol%) had comparatively little effect on microstructure, except for changes in spinel phase composition, in the traditional ZnO based formulation including Sb_2O_3; they were able to achieve α values of 37–46. It would be interesting to explore the effect of Sb_2O_3 and five valent oxide additions on the electrical properties of these ZnO–SnO_2 based ceramics.

Electrical breakdown fields are summarised in Fig. 5. E_b depends critically on composition but is less sensitive to sintering temperature. The breakdown field E_b is almost independent of sintering temperature, but increases almost linearly with SnO_2 content from 3800 to approximately 11 000 V/cm (in samples prepared with 20% SnO_2). At the same time it was found that the leakage current I_L increases slightly with increasing sintering temperature, but decreases as the SnO_2 content increases. For example in samples sintered at 1250 °C, I_L decreases from 9 μA at 15% SnO_2 to 4 μA at 20% SnO_2. These leakage currents are lower than those reported by Bernik and Daneu for SnO_2 doped ZnO varistors,[10] and the E_B values achieved here for the mixed ZnO–SnO_2 varistors are at least comparable with those reported by Santos et al. for SnO_2 varistors.[8,9] Thus whilst the mixed ZnO–SnO_2 varistors exhibit slightly lower α values than some competing formulations, they do have attractive breakdown fields and leakage currents and can be fabricated relatively easily.

On the basis of C–V measurements, Bernik and Daneu[10] deduced that substitution of Sb_2O_3 by SnO_2 gives rise to a strong donor effect causing a slight increase in leakage current. Preliminary CV investigations of SBSN samples by Lee[12] indicate a similar mechanism when SnO_2 replaces ZnO.

4. Conclusions

The densities of ZnO–SnO_2 based varistors increased with SnO_2 content, but decreased with increase in sintering temperature. The microstructures of all samples comprised ZnO primary grains, Zn_2SnO_4 spinel and very small bismuth rich phases at the grain boundaries. As SnO_2 replaced ZnO, the size of the ZnO grains decreased and the spinel became the dominant phase. From I–V measurements, the non-linear coefficients were found to be in the range 24–32. The α values were almost independent of SnO_2 content up to 15 mol%, but increased at higher levels of tin replacement. For all compositions the α values decreased with increasing sintering temperature; the maximum α value was achieved for samples prepared with 20 mol% SnO_2 sintered at 1200 °C. Breakdown fields were in the range 3000–11 000 V/cm and increased with increasing tin content. Leakage currents were in the range 1–11 μA and tended to decrease with increasing SnO_2 content. Related studies suggest that tin substitution for Zn has a strong donor effect.

Thus replacement of Zn by Sn in ceramic varistors of model formulation has a dramatic effect on the microstructure with the development of extensive regions of Zn_2SnO_4 spinel. Whilst the non-linear coefficients are not quite as high as those in the best ZnO varistors, the E_B values are uniformly high and leakage currents low, making them potentially attractive for further investigation and evaluation.

References

1. Matsuoka, M., Non-ohmic properties of zinc oxide ceramics. *Jpn. J. Appl. Phys*, 1971, **10**, 736–746.
2. Gupta, T. K., Microstructural engineering through donor and acceptor doping in the grain and grain boundary of a polycrystalline semiconducting ceramic. *J. Mat. Res.*, 1992, **12**, 3280–3295.
3. Makarow, V. and Trontelj, M., Novel varistor materials based on tungsten oxide. *J. Mat. Lett.*, 1994, **13**, 937–939.
4. Yamaoka, N., Masuyama, M. and Fukui, M., $SrTiO_3$ based boundary-layer capacitor having varistor characteristics. *Am. Ceram. Soc. Bull*, 1983, **62**, 698.

5. Yan, J. F. and Rhodes, W. W., Preparation and properties of TiO_2 varistors. *Appl. Phys. Lett*., 1982, **40**, 536–537.
6. Yang, S. L. and Wu, J. M., Effects of Nb_2O_5 in (Ba,Bi,Nb)-added TiO_2 ceramic varistors. *J. Mat. Res*., 1995, **10**, 345–352.
7. Beuno, P. R., Camargo, E. and Longo, E., Effect of Cr_2O_3 in varistor behaviour of TiO2. *J. Mater. Sci*., 1996, **15**, 2048–2050.
8. Pianaro, S. A., Beuno, P. R., Longo, E. and Varela, J. A., A new SnO_2 based varistor system. *Mater. Sci. Lett*., 1995, **14**, 692–694.
9. Santos, M. R. C., Beuno, P. R., Longo, E. and Varela, J. A., Effect of oxidizing and reducing atmosphere on the electrical properties of dense SnO_2-based varistors. *J. Europ. Ceram. Soc*., 2001, **21**, 161–167.
10. Bernik, S. and Daneu, N., Characteristics of SnO_2-doped ZnO-based varistor ceramics. *J. Eur. Ceram. Soc*., 2001, **21**, 1879–1882.
11. Gupta, T. K., Application of zinc oxide varistors. *J. Am. Ceram. Soc*., 1990, **73**, 1817–1840.
12. Lee, M-H. J., MPhil Thesis, University of Manchester Institute of Science and Technology, 2001.